PROPERTIES, DIGITAL IMPLEMENTATION, APPLICATIONS, AND SELF IMAGE PHENOMENA OF THE GYRATOR TRANSFORM

Soo-Chang Pei and Jian-Jiun Ding

Department of Electrical Engineering, National Taiwan University,
No. 1, Sec. 4, Roosevelt Rd., 10617, Taipei, Taiwan, R.O.C
TEL: 886-2-23635251-321, Fax: 886-2-23671909, Email: pei@cc.ee.ntu.edu.tw, djj@cc.ee.ntu.edu.tw

ABSTRACT

The gyrator transform was introduced in recent years and useful for image processing. As the fractional Fourier transform, the gyrator transform can also be viewed as an extension of the Fourier analysis. In this paper, we discuss the digital implementation algorithms of the gyrator transform. We also discuss the eigenfunctions and the self-imaging phenomena of the gyrator transform. Many properties, such as the differential and dilation preservation properties, are also discussed. We also discuss the possible applications of the gyrator transform in filter design and signal sampling.

1. INTRUDUCTION

The **gyrator transform** [1][2][3] is a new operation introduced by Rodrigo, Alieva, and Calvo in 2007. It is defined as:

$$G_\alpha(u,v)=O_{gy}^{\alpha}\left[g(x,y)\right]= \frac{|\csc\alpha|}{2\pi}\int_{-\infty}^{\infty}\int_{-\infty}^{\infty}\exp\left(j\frac{(uv+xy)\cos\alpha-(uy+vx)}{\sin\alpha}\right)g(x,y)\,dxdy \tag{1}$$

When $\alpha=0$, it becomes the identity operation. When $\alpha=\pi/2$, it becomes the Fourier transform (FT) together with the axis exchange operation. The gyrator transform has additivity and periodic properties:

$$O_{gy}^{\alpha}\left\{O_{gy}^{\beta}\left[g(x,y)\right]\right\}=O_{gy}^{\alpha+\beta}\left[g(x,y)\right], \tag{2}$$

$$O_{gy}^{\alpha+2\pi}\left[g(x,y)\right]=O_{gy}^{\alpha}\left[g(x,y)\right]. \tag{3}$$

The gyrator transform was found to be useful in optics [1][2][3], image processing [1][5], and encryption [6].

The gyrator transform is very similar to the 2-D fractional Fourier transform (2-D FRFT) [4]:

$$FRFT_{\alpha,\gamma}\left[g(x,y)\right]=\frac{\sqrt{1-j\cot\alpha}\sqrt{1-j\cot\gamma}}{2\pi}e^{\frac{j}{2}(u^2\cot\alpha+v^2\cot\gamma)}\times \int_{-\infty}^{\infty}\int_{-\infty}^{\infty}e^{-j(ux\csc\alpha+vy\csc\gamma)}e^{\frac{j}{2}(x^2\cot\alpha+y^2\cot\gamma)}g(x,y)\,dxdy \tag{4}$$

Both the FRFT and the gyrator transform can be viewed as the extensions of the Fourier analysis. Thus, as the FRFT [4], we believe that the gyrator transform can also be very useful in signal processing. The motivation of this paper is to explore the implementation algorithms and the possible signal processing applications of the gyrator transform.

First, in Section 2, we describe two efficient ways to digitally implement the gyrator transform. Then, we derive several properties in Section 3. In Section 4, we discuss the eigenfunctions of the gyrator transform and use them to discuss the self-imaging phenomena of the optical system related to the gyrator transform. In Section 5, we show that the gyrator transform can be useful in signal sampling, filter design, and communication.

2. DIGITAL IMPLEMENTATION

The optical implementation of the gyrator transform is described in [2]. Here, we discuss the digital implementation method. There are many ways to implement the gyrator transform digitally. We describe two of them.

(Implementation Method 1):
Suppose that the sampling intervals in the space and the frequency domain are Δ_s, Δ_ω, respectively:

$$g_1[m,n]=g(m\Delta_s,n\Delta_s)\quad G_{\alpha,1}[p,q]=G_\alpha(p\Delta_\omega,q\Delta_\omega). \tag{5}$$

Then (1) can be rewritten as:

$$G_{\alpha,1}(p,q)=\Delta_s^2|\csc\alpha|/2\pi\times \sum_m\sum_n\exp\left(j\frac{(pq\Delta_\omega^2+mn\Delta_s^2)\cos\alpha-(pn+qm)\Delta_s\Delta_\omega}{\sin\alpha}\right)g_1[m,n] \tag{6}$$

Therefore, if we choose Δ_s and Δ_ω properly such that

$$\Delta_s\Delta_\omega=2\pi\sin\alpha/N, \tag{7}$$

where N is some integer and N should be larger than the number of sampling points in x-axis and y-axis. Then the gyrator transform can be implemented by:

$$\text{(Step 1)}\quad g_2[m,n]=e^{jmn\Delta_s^2\cot\alpha}g_1[m,n], \tag{8}$$

$$\text{(Step 2)}\quad G_{\alpha,2}[p,q]=\sum_m\sum_n\exp\left(-j2\pi\frac{pm+qn}{N}\right)g_2[m,n], \quad\text{(by the discrete Fourier transform (DFT))} \tag{9}$$

$$\text{(Step 3)}\quad G_{\alpha,1}[p,q]=\Delta_s^2\frac{|\csc\alpha|}{2\pi}e^{jpq\Delta_\omega^2\cot\alpha}G_{\alpha,3}[p,q], \tag{10}$$

$$\text{where}\quad G_{\alpha,3}[p,q]=G_{\alpha,2}[q,p]. \tag{11}$$

In Fig. 1, we show the results of using Method 1 to perform the gyrator transform for 256×256 Lena image. The running time for each figure is less than 0.5 sec (using PC and Matlab). In Fig. 2, we show the results when varying the values of N in (7). When N is larger, the results can be a little clearer.

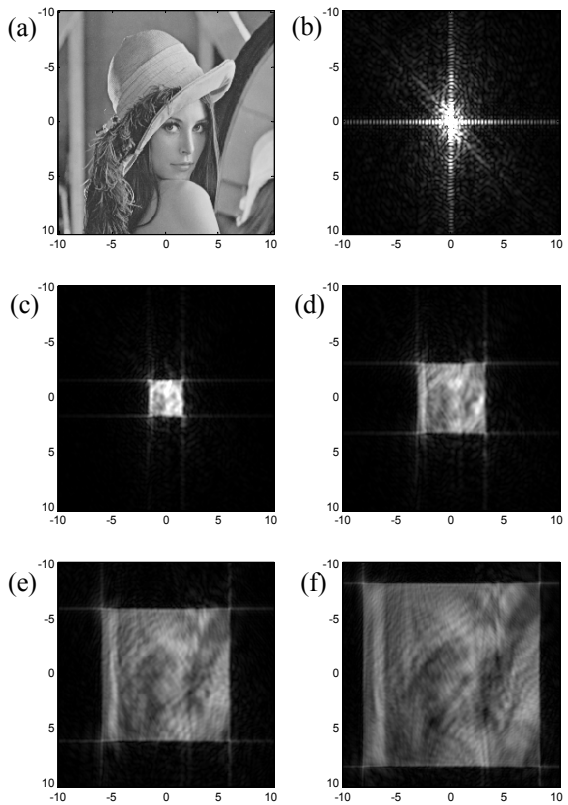

Fig. 1 The gyrator transform for 256×256 Lena image (choose $N = 500$). (a) Original image, (b) $\alpha = 0.5\pi$, (c) $\alpha = 0.45\pi$, (d) $\alpha = 0.4\pi$, (e) $\alpha = 0.3\pi$, (f) $\alpha = 0.2\pi$.

(Implementation Method 2):

Sometimes, Δ_s and Δ_ω are fixed and we cannot adjust them to satisfy (7). In this case, we can use the fact that

$$-2(pn+qm) = (p-n)^2 + (q-m)^2 - \left(p^2+q^2+m^2+n^2\right). \quad (12)$$

Thus, we can use the following process to implement the gyrator transform:

$$\text{(Step 1)}\ g_2[m,n] = e^{\frac{-j}{2}(m^2+n^2)\Delta_s\Delta_\omega \csc\alpha} e^{jmn\Delta_s^2\cot\alpha} g_1[m,n] \quad (13)$$

$$\text{(Step 2)}\ G_{\alpha,2}[p,q]$$

$$= \sum_m\sum_n \exp\left(\frac{j}{2}[(p-m)^2+(q-n)^2]\Delta_s\Delta_\omega\csc\alpha\right) g_2[m,n]$$

$$= \exp\left(j[p^2+q^2]\Delta_s\Delta_\omega\csc\alpha/2\right) * g_2[p,q], \quad (14)$$

$$\text{(Step 3)}\ G_{\alpha,1}[p,q] = \frac{|\csc\alpha|}{2\pi}\Delta_s^2 e^{\frac{-j}{2}(p^2+q^2)\Delta_s\Delta_\omega\csc\alpha} e^{jpq\Delta_\omega^2\cot\alpha} G_{\alpha,2}[q,p]. \quad (15)$$

Compared with Method 1, Method 2 uses chirp convolution instead of performing the DFT in Step 2.

Although there are other digital implementation methods, the algorithms described above can avoid geometric twisting or geometric rotation operations. In digital implementation, geometric twisting and rotation needs interpolation operations, which reduce accuracy

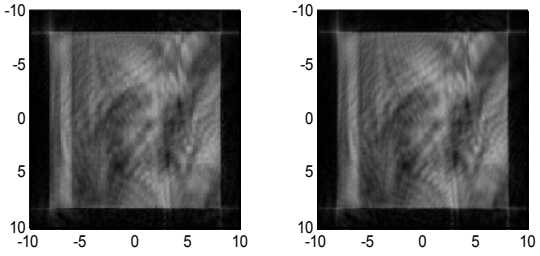

Fig. 2 The gyrator transform for Lena image when $\alpha = 0.2\pi$, (a) $N = 260$, (b) $N = 1200$.

3. PROPERTIES

In [1], several properties of the gyrator transform were derived, including the shifting, scaling, modulation, and energy preservation properties. In the following, using the methods similar to those in [12][13], we derive other properties of the gyrator transform. We use $O_{gy}{}^{\alpha}$ to denote the gyrator transform operation with order α and use $G_\alpha(u, v)$ to denote the gyrator transform of $g(x, y)$:

$$G_\alpha(u,v) = O_{gy}^{\alpha}[g(x,y)]. \quad (16)$$

(A) Multiplication Property

$$O_{gy}^{\alpha}[xg(x,y)] = j\frac{\partial}{\partial v}G_\alpha(u,v)\sin\alpha + uG_\alpha(u,v)\cos\alpha. \quad (17)$$

$$O_{gy}^{\alpha}[yg(x,y)] = j\frac{\partial}{\partial u}G_\alpha(u,v)\sin\alpha + vG_\alpha(u,v)\cos\alpha. \quad (18)$$

(Proof of (17)): From (1),

$$\frac{\partial G_\alpha(u,v)}{\partial v}$$

$$= \frac{|\csc\alpha|}{2\pi}\int_{-\infty}^{\infty}\int_{-\infty}^{\infty}(ju\cot\alpha - jx\csc\alpha)e^{j\frac{(uv+xy)\cos\alpha-(uy+vx)}{\sin\alpha}} g(x,y)\,dxdy$$

$$= juG_\alpha(u,v)\cot\alpha - jO_{gy}^{\alpha}[xg(x,y)]\csc\alpha. \quad (19)$$

Multiplying both sides by $j\sin\alpha$, we obtain (17). #

(B) Differentiation Property

$$O_{gy}^{\alpha}\left[\frac{\partial}{\partial x}g(x,y)\right] = \frac{\partial}{\partial u}G_\alpha(u,v)\cos\alpha + jvG_\alpha(u,v)\sin\alpha, \quad (20)$$

$$O_{gy}^{\alpha}\left[\frac{\partial}{\partial y}g(x,y)\right] = \frac{\partial}{\partial v}G_\alpha(u,v)\cos\alpha + juG_\alpha(u,v)\sin\alpha. \quad (21)$$

(Proof): $g(x,y) = O_{gy}^{-\alpha}[G_\alpha(u,v)]$

$$= \frac{|\csc\alpha|}{2\pi}\int_{-\infty}^{\infty}\int_{-\infty}^{\infty} e^{j\frac{-(xy+uv)\cos\alpha+(xv+uy)}{\sin\alpha}} G_\alpha(u,v)\,dudv,$$

$$\frac{\partial g(x,y)}{\partial x} = \frac{|\csc\alpha|}{2\pi}\times$$

$$\int_{-\infty}^{\infty}\int_{-\infty}^{\infty} j(v\csc\alpha - y\cot\alpha)e^{j\frac{-(xy+uv)\cos\alpha+(xv+uy)}{\sin\alpha}} G_\alpha(u,v)\,dudv,$$

$$\frac{\partial g(x,y)}{\partial x} = j\csc\alpha O_{gy}^{-\alpha}(vG_\alpha(u,v)) - jy\cot\alpha g(x,y),$$

$$O_{gy}^{\alpha}\left(\frac{\partial g(x,y)}{\partial x}\right) = jv\csc\alpha G_\alpha(u,v) - j\cot\alpha O_{gy}^{\alpha}(yg(x,y)). \quad (22)$$

Then, we substitute (18) into (22). After some computation, we obtain (20). #

(C) Conjugation Property

$$O_{gy}^{\alpha}\left[g^{*}(x,y)\right]=G_{-\alpha}^{*}(u,v). \tag{23}$$

(D) Relation with the Scaling operation:

Note that, from (1),

$$\begin{aligned}
&G_{\alpha}(u,v)\\
&=\frac{e^{-juv\tan\alpha}}{2\pi|\sin\alpha|}\int_{-\infty}^{\infty}\int_{-\infty}^{\infty}e^{juv\cot\alpha(1+\tan^{2}\alpha)}e^{-j(uy+vx)\csc\alpha}e^{jxy\cot\alpha}\,g(x,y)\,dxdy\\
&=\frac{e^{-juv\tan\alpha}}{2\pi|\sin\alpha|}\int_{-\infty}^{\infty}\int_{-\infty}^{\infty}e^{j\frac{uv}{\sin\alpha\cos\alpha}}e^{-j\frac{uy+vx}{\sin\alpha}}e^{j\frac{xy\cos\alpha}{\sin\alpha}}\,g(x,y)\,dxdy\\
&=\frac{e^{-juv\tan\alpha}}{2\pi|\sin\alpha|}\int_{-\infty}^{\infty}\int_{-\infty}^{\infty}\exp\left(j\frac{(u-x\cos\alpha)(v-y\cos\alpha)}{\sin\alpha\cos\alpha}\right)g(x,y)\,dxdy\\
&=\frac{e^{-juv\tan\alpha}}{2\pi|\sin\alpha\cos^{2}\alpha|}\int_{-\infty}^{\infty}\int_{-\infty}^{\infty}\exp\left(j\frac{(u-x)(v-y)}{\sin\alpha\cos\alpha}\right)g\left(\frac{x}{\cos\alpha},\frac{y}{\cos\alpha}\right)dxdy\,.
\end{aligned}$$

Therefore,

$$\left|G_{\alpha}(u,v)\right|=\frac{\left|\exp\left(j\frac{2xy}{\sin(2\alpha)}\right)*g\left(\frac{x}{\cos\alpha},\frac{y}{\cos\alpha}\right)\right|}{\pi|\sin(2\alpha)\cos\alpha|} \tag{24}$$

That is, the gyrator transform with parameter α has a very close relation with $g(x/\cos\alpha, y/\cos\alpha)$. This can explain why in Fig. 1 the results of the gyrator transform seems to be the scaling of the original image especially when α is small.

(E) Relations between the Gyrator Transform and the FRFT.

$$G_{\alpha}(u,v)=O_{rot}^{-\pi/4}\left\{FRFT_{\alpha,-\alpha}\left[O_{rot}^{\pi/4}\left[g(x,y)\right]\right]\right\}, \tag{25}$$

where $O_{rot}^{\phi}\left[g(x,y)\right]$ means the geometric rotation operation:

$$O_{rot}^{\phi}\left[g(x,y)\right]=g\left(x\cos\phi-y\sin\phi,x\sin\phi+y\cos\phi\right). \tag{26}$$

4. EIGENFUNCTIONS AND SELF-IMAGING PHENOMENA

4.1 Eigenfunctions

[Theorem 1] If $e(x, y)$ is an eigenvector of the 2-D FRFT with parameters $(\alpha, -\alpha)$ and the eigenvalue is λ:

$$FRFT_{\alpha,-\alpha}\left[e(x,y)\right]=\lambda e(x,y), \tag{27}$$

then

$$f(x,y)=e\left(\frac{x+y}{\sqrt{2}},\frac{-x+y}{\sqrt{2}}\right) \tag{28}$$

is the eigenvector of the gyrator transform and the eigenvalue is also λ:

$$O_{gy}^{\alpha}\left[f(x,y)\right]=\lambda f(x,y). \tag{29}$$

In other words **the eigenfunctions of the gyrator transform is the rotation of those of the FRFT with 45 degree**:

$$f(x,y)=O_{rot}^{-\pi/4}\left[e(x,y)\right]. \tag{30}$$

(Proof): From the relation between the gyrator transform and the 2-D FRFT in (25),

$$\begin{aligned}
&O_{gy}^{\alpha}\left[f(x,y)\right]=O_{rot}^{-\pi/4}\left\{FRFT_{\alpha,-\alpha}\left[O_{rot}^{\pi/4}\left[f(x,y)\right]\right]\right\}\\
&=O_{rot}^{-\pi/4}\left\{FRFT_{\alpha,-\alpha}\left[e(x,y)\right]\right\}=\lambda O_{rot}^{-\pi/4}\left\{e(x,y)\right\}. \qquad \#
\end{aligned}$$

[Corollary 1] From Theorem 1, we can derive the eigenfunctions of the gyrator transform from those of the FRFT. For example, 2-D Hermite-Gaussians are the eigenfunctions of the 2-D FRFT:

$$HG_{m,n}(x,y)=e^{-\frac{x^{2}+y^{2}}{2}}h_{m}(x)h_{n}(y), \tag{31}$$

where $h_m(x)$ is the m^{th} order Hermite polynomial, and

$$FRFT_{\alpha,-\alpha}\left[HG_{m,n}(x,y)\right]=e^{j\alpha(n-m)}HG_{m,n}(x,y). \tag{32}$$

Therefore, from Theorem 1, the following function will be the eigenfunction of the gyrator transform:

$$\Psi_{m,n}(x,y)=e^{-\frac{x^{2}+y^{2}}{2}}h_{m}\left(\frac{x+y}{\sqrt{2}}\right)h_{n}\left(\frac{-x+y}{\sqrt{2}}\right) \tag{33}$$

and

$$O_{gy}^{\alpha}\left[\Psi_{m,n}(x,y)\right]=e^{j\alpha(n-m)}\Psi_{m,n}(x,y). \tag{34}$$

[Corollary 2] Moreover, from (34), $\lambda = \exp(j\alpha(n-m))$. Since when $m-n$ is fixed, the corresponding eigenvalue is the same, thus, if we do linear combination for (38):

$$\Phi(x,y)=e^{-\frac{x^{2}+y^{2}}{2}}\sum_{k=0}^{m}a_{k}h_{m}\left(\frac{x+y}{\sqrt{2}}\right)h_{k-m}\left(\frac{-x+y}{\sqrt{2}}\right) \tag{35}$$

then Φ(x, y) is also an eigenfunction of the gyrator transform and the corresponding eigenvalue is $\exp(-j\alpha k)$.

4.2 Self-Imaging Phenomena

Since the gyrator transform can be modelled by optical systems [2][3], therefore, the eigenfunctions of the gyrator transform can causes the self-imaging phenomena of these optical systems.

However, for analyzing the self-imaging phenomena, the constraint can be more relaxed. Since in optics, only the intensity is observed and the difference of scaling is tolerated when discussing the self-imaging phenomena, therefore, if

$$O_{gy}^{\alpha}\left[s(x,y)\right]=z(u,v), \text{ and } \left|z(x,y)\right|=\tau\left|s(\sigma x,\sigma y)\right| \tag{36}$$

then $s(x, y)$ will also cause the self-imaging phenomena for the optical system that can be implemented by the gyrator transform.

In addition to (25), the gyrator transform can also be expressed as a combination of the rotation operations and the linear canonical transform (LCT) if the difference of phase and scaling is ignored:

$$K_{\alpha}(u,v)=O_{rot}^{-\pi/4}\left\{LCT_{(a,b,c,d),(a,-b,-c,d)}\left[O_{rot}^{\pi/4}\left[g(x,y)\right]\right]\right\}, \tag{37}$$

$$G_{\alpha}(u,v)=e^{-j\left(\tan\alpha+\frac{2bc}{\sin(\alpha/2)}\right)uv}K_{\alpha}\left(\frac{au}{\cos\alpha},\frac{av}{\cos\alpha}\right), \tag{38}$$

where $O_{rot}^{\phi}\left[g(x,y)\right]$ is defined in (26) and the LCT is defined as [7]:

$$\begin{aligned}
&LCT_{(a,b,c,d,a_1,b_1,c_1,d_1)}\left[g(x,y)\right]=\frac{1}{2\pi\sqrt{-bb_1}}e^{j\left(\frac{d}{2b}u^{2}+\frac{d_1}{2b_1}v^{2}\right)}\times\\
&\int_{-\infty}^{\infty}\int_{-\infty}^{\infty}e^{-j\left(\frac{ux}{b}+\frac{vy}{b_1}\right)}e^{j\left(\frac{a}{2b}x^{2}+\frac{a_1}{2b_1}y^{2}\right)}\,g(x,y)\,dxdy\,,
\end{aligned} \tag{39}$$

and the parameters in (37) should satisfy

$$a : b = \cos\alpha : \sin\alpha \quad \text{and} \quad ad - bc = 1. \tag{40}$$

Therefore, if $p(x, y)$ is the eigenfunction of the 2-D LCT with parameter $\{a, b, c, d, a, -b, -c, d\}$:

$$LCT_{(a,b,c,d,a_1,b_1,c_1,d_1)}\left[p(x,y)\right] = \lambda\, p(x,y) \tag{41}$$

after performing geometric rotation for $p(x, y)$:

$$q(x,y) = O_{rot}^{-\pi/4}\left[p(x,y)\right] = p\left(\frac{x+y}{\sqrt{2}}, \frac{-x+y}{\sqrt{2}}\right), \tag{42}$$

then, from (42) and (43),

$$Q_\alpha(u,v) = O_{gy}^{\alpha}\left[q(x,y)\right] = \lambda e^{-j\left(\tan\alpha + \frac{2bc}{\sin(\alpha/2)}\right)uv} q\left(\frac{au}{\cos\alpha}, \frac{av}{\cos\alpha}\right), \tag{43}$$

$$\left|Q_\alpha(u,v)\right| = \left|q(au/\cos\alpha, av/\cos\alpha)\right|. \tag{44}$$

Since $q(x, y)$ and $Q_\alpha(u, v)$ only differ in scaling, $q(x, y)$, i.e., **the rotation of the eigenfunctions of the 2-D LCT, will case the self-imaging phenomena of the gyrator transform**. From [8], the eigenfunctions of the LCT are Hermite-Gaussian functions, impulse trains, and fractals together with scaling, chirp multiplication, and chirp convolution. After rotating them by 45 degree, as in (42), these functions can all cause the self-imaging phenomena of the gyrator transform.

5. APPLICATIONS

As the FRFT, the gyrator transform can be viewed as an extension of Fourier analysis. Therefore, many applications of the Fourier transform and the FRFT can also be viewed as the applications of the gyrator transform. The applications of the gyrator transform in **optics**, **image processing** and **encryption** were introduced in [1][2][3][5][6]. Here, we discuss other possible applications of the gyrator transform.

5.1 Sampling Theory

Suppose that a signal $g(x, y)$ is limited in the gyrator transform domain:

$$G_\alpha(u,v) = 0 \quad \text{when } |u| > B_1, \quad |v| > B_2. \tag{45}$$

Note that, if a signal satisfies (45), then it is impossible to be band-limited in the frequency transform and we cannot use the conventional Shannon's Sampling Theorem to sample the signal. However, we can use the gyrator transform to sample it. If we performing sampling for $g(x, y)$:

$$g_1(x,y) = \sum_m \sum_n g(m\Delta_x, n\Delta_y)\,\delta(x - m\Delta_x, y - n\Delta_y), \tag{46}$$

then the gyrator transform of $g_1(x, y)$ is

$$G_{1,\alpha}(u,v) = \frac{|\csc\alpha|}{2\pi} e^{juv\cot\alpha} \int_{-\infty}^{\infty}\int_{-\infty}^{\infty} e^{-j\frac{(uy+vx)}{\sin\alpha}} e^{jxy\cot\alpha} \sum_m \sum_n g(m\Delta_x, n\Delta_y)\,\delta(x - m\Delta_x, y - n\Delta_y)\,dxdy. \tag{47}$$

Then, since from the Fourier transform pair for the comb function [14]

$$\int_{-\infty}^{\infty}\int_{-\infty}^{\infty} e^{-j2\pi(ux+vy)} \sum_m \sum_n f(m\Delta_x, n\Delta_y)\,\delta(x - m\Delta_x, y - n\Delta_y)\,dxdy = \frac{1}{\Delta_x\Delta_y} \sum_m \sum_n F(u - m/\Delta_x, v - n/\Delta_y), \tag{48}$$

$$\int_{-\infty}^{\infty}\int_{-\infty}^{\infty} e^{-j\frac{(vx+uy)}{\sin\alpha}} \sum_m \sum_n f(m\Delta_x, n\Delta_y)\,\delta(x - m\Delta_x, y - n\Delta_y)\,dxdy = \frac{1}{\Delta_x\Delta_y} \sum_m \sum_n F\left(\frac{v}{2\pi\sin\alpha} - \frac{m}{\Delta_x}, \frac{u}{2\pi\sin\alpha} - \frac{n}{\Delta_y}\right). \tag{49}$$

After substituting $\exp(jxy\cot\alpha)g(x, y)$ into $f(x, y)$ in (49), (47) can be rewritten as

$$G_{1,\alpha}(u,v) = \frac{|\csc\alpha|}{2\pi\Delta_x\Delta_y} e^{juv\cot\alpha} \sum_m \sum_n F\left(\frac{v}{2\pi\sin\alpha} - \frac{m}{\Delta_x}, \frac{u}{2\pi\sin\alpha} - \frac{n}{\Delta_y}\right) \tag{50}$$

where $F(u,v) = \int_{-\infty}^{\infty}\int_{-\infty}^{\infty} e^{-j2\pi(ux+vy)} e^{jxy\cot\alpha} g(x,y)\,dxdy$

$$= 2\pi\,|\sin\alpha|\, e^{-juv4\pi^2\sin^2\alpha\cot\alpha} G_\alpha(2\pi v\sin\alpha, 2\pi u\sin\alpha). \tag{51}$$

Therefore, the relation between the gyrator transform of $g(x, y)$ and that of $g_1(x, y)$ is:

$$G_{1,\alpha}(u,v) = \frac{1}{\Delta_x\Delta_y} \sum_m \sum_n G_\alpha\left(u - 2\pi\frac{n}{\Delta_y}\sin\alpha, v - 2\pi\frac{m}{\Delta_x}\sin\alpha\right) e^{j\left(uv - \left(u - 2\pi\frac{n}{\Delta_y}\sin\alpha\right)\left(v - 2\pi\frac{m}{\Delta_x}\sin\alpha\right)\right)\cot\alpha}. \tag{52}$$

From (52), if we choose the sampling intervals properly:

$$\Delta_x < \frac{\pi}{B_2}\sin\alpha \quad \text{and} \quad \Delta_y < \frac{\pi}{B_1}\sin\alpha, \tag{53}$$

then we can reconstruct $g(x, y)$ from $g_1(x, y)$ by placing a lowpass mask in the gyrator transform domain:

$$G_\alpha(u,v) = \Delta_x\Delta_y M(u,v) G_{1,\alpha}(u,v), \tag{54}$$

$$g(x,y) = O_{gy}^{-\alpha}\left\{M(u,v) G_{1,\alpha}(u,v)\right\}, \tag{55}$$

$$M(u, v) = 1 \text{ if } |u| < C_1 \text{ and } |v| < C_2, \tag{56}$$

$$M(u, v) = 0 \text{ otherwise}, \tag{57}$$

$$B_1 < C_1 < \frac{2\pi}{\Delta_y}\sin\alpha - B_1, \quad B_2 < C_2 < \frac{2\pi}{\Delta_x}\sin\alpha - B_2. \tag{58}$$

Therefore, even if a signal is not limited in the frequency domain, if it satisfies (45), we can use the gyrator transform and the above process to sample and reconstruct the signal.

5.2 Filter Design

As the FT and the FRFT, the gyrator transform is also useful for filter design. That is, we can perform the gyrator transform for a noise-interfered signal, then multiply the result by a transfer function, and then perform the inverse gyrator transform to recover the original signal:

$$g_o(x,y) = O_{gy}^{-\alpha}\left\{H(u,v) O_{gy}^{\alpha}\left[g_i(x,y)\right]\right\}. \tag{59}$$

Note that the reconstruction process in (55) is a special case of the filter designed by the gyrator transform.

As the filter designed by the FRFT, which is suitable for filtering the chirp noise [10], the filter designed by the gyrator transform can be used for filtering the noise that has the form of the summation of

$$\exp(j\tau_1 xy + j\tau_2 x + j\tau_3 y). \tag{60}$$

Moreover, analogous to the applications of the filter designed by the FRFT, the filter designed by the gyrator transform is also useful for space-variant pattern recognition, edge detection, and wavelet analysis.

(a) Original image + noise (b) 2-D FT for (a)

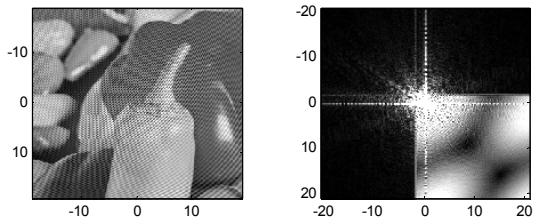

(c) gyrator transform for (a) (d) Reconstructed signal

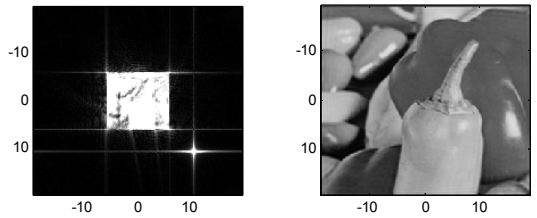

Fig. 3 The simulation of using the gyrator transform for filter design.

For example, in Fig. 3(a), the signal is interfered by a quadratic phase noise. If we perform the 2-D Fourier transform for Fig. 3(a), the noise part and the signal part cannot be separated, as in Fig. 3(b). By contrast, if we perform the gyrator transform for Fig. 3(a), the signal part and the noise part can be well separated, as in Fig. 3(c). After performing the inverse gyrator transform, the original image is recovered. See Fig. 3(d).

5.3 Wave Propagation Analysis

We have discussed that the gyrator transform is useful for analyzing the self-imaging phenomena in optics in Section 4.2. Similarly, the gyrator transform is also useful for analyzing other electromagnetic wave propagation phenomena, such as radar system analysis and gradient index filter system analysis. The gyrator transform is useful for analyzing the resonance phenomena of these systems.

6. CONCLUSIONS

In this paper, we derive the properties and eigenfunction of the gyrator transform. We also discuss its digital implementation algorithms and describe its applications for filter design, sampling theory, and optical system analysis. As the FRFT, the gyrator transform will become a useful tool in signal analysis.

REFERENCES

[1] J. A. Rodrigo, T. Alieva, and M. L. Calvo, "Gyrator transform: properties and applications," *Opt. Express*, vol. 15, pp. 2190-2203, 2007.

[2] J. A. Rodrigo, T. Alieva, and M. L. Calvo, "Experimental implementation of the gyrator transform," *J. Opt. Soc. Am. A*, vol. 24, no. 10, pp. 3135-3139, Oct. 2007.

[3] K. B. Wolf and T. Alieva, "Rotation and gyrator of finite two-dimensional modes," *J. Opt. Soc. Am. A*, vol. 25, no. 2, pp. 265-270, Feb. 2008.

[4] H. M. Ozaktas, Z. Zalevsky, and M. A. Kutay, *The Fractional Fourier Transform with Applications in Optics and Signal Processing*, New York, John Wiley & Sons, 2000.

[5] J. A. Rodrigo, T. Alieva, and M. L. Calvo, "Gyrator transform for image processing," *Opt. Commun.*, vol. 278, pp. 279-284, 2007.

[6] H. Li and Y. Yang, "Information security system based on interative multiple-phase retrieval in gyrator domain," *Opt. Laser Technol.*, vol. 40,pp. 962-966, 2008.

[7] K. B. Wolf, "*Integral Transforms in Science and Engineering*," Ch. 9: Canonical transforms, New York, Plenum Press, 1979.

[8] S. C. Pei and J. J. Ding, "Eigenfunctions of linear canonical transform," *IEEE Trans. Signal Processing*, vol. 50, no. 1, pp. 11-26, Jan. 2002.

[9] X. G. Xia, "On bandlimited signals with fractional Fourier transform," *IEEE Signal Processing Letters*, vol. 3, no. 3, pp. 72-74, Mar. 1996.

[10] M. A. Kutay, H. M. Ozaktas, O. Arikan, and L. Onural, "Optimal filter in fractional Fourier domains," *IEEE Trans. Signal Processing*, vol. 45, no. 5, pp. 1129-1143, May 1997.

[11] R. N. Bracewell, *The Fourier Transform and Its Applications*, 3rd ed., Boston, McGraw Hill, 2000.

[12] T. Alieva and M. J. Bastiaans, "Properties of the linear canonical integral transformation," *J. Opt. Soc. Am. A*, vol. 24, no. 11, pp. 3658-3665, Nov. 2007.

[13] M. J. Bastiaans and T. Alieva, "First-order optical systems with unimodular eigenvalues," *J. Opt. Soc. Am. A*, vol. 23, no. 8, pp. 1875-1883, Aug. 2006.

[14] T. Alieva and M. J. Bastiaans, "Mode mapping in paraxial lossless optics," *Opt. Lett.*, vol. 30, no. 12, pp. 1461-1463, June 2005.

[15] T. Alieva and M. J. Bastiaans, "Orthonormal mode sets for the two-dimensional fractional Fourier transformation," *Opt. Lett.*, vol. 32, no. 10, pp. 1226-1228, May 2007.